ACKNOWLEDGMENT

The authors would like to thank Prof. G. A. Deschamps for suggesting the problem and for spending many hours of discussion. In addition, the generous assistance rendered by Prof. J. D. Dyson is gratefully appreciated.

REFERENCES

[1] J. D. Jackson, *Classical Electrodynamics.* New York: Wiley, 1962.

[2] V. H. Rumsey, "A new way of solving Maxwell's equations," *IRE Trans. Antennas and Propagation*, vol. AP-9, pp. 461–465, September 1961.

[3] J. D. Dyson, "The equiangular spiral antenna," *IRE Trans. Antennas and Propagation*, vol. AP-7, pp. 181–187, April 1959.

[4] J. D. Dyson and P. E. Mayes, "New circularly-polarized frequency-independent antennas with conical beam or omnidirectional patterns," *IRE Trans. Antennas and Propagation*, vol. AP-9, pp. 334–342, July 1961.

[5] R. Sivan-Sussman, "Various modes of the equiangular spiral antenna," *IEEE Trans. Antennas and Propagation*, vol. AP-11, pp. 533–539, September 1963.

[6] B. R. S. Cheo, V. H. Rumsey, and W. J. Welch, "A solution to the frequency-independent antenna problems," *IRE Trans. Antennas and Propagation*, vol. AP-9, pp. 527–534, November 1961.

[7] R. Mittra and P. W. Klock, "A theoretical study of the conical spiral antenna," *Proc. Symp. on Electromagnetic Theory and Antennas* (Delft, Netherlands). New York: Pergamon, 1967.

[8] S. R. Laxpati and R. Mittra, "A study of the equiangular spiral antenna," Antenna Lab., University of Illinois, Urbana, Tech. Rept. 65-20, AFAL-TR-65-330, February 1966.

[9] Y. S. Yeh and K. K. Mei, "Theory of conical equiangular-spiral antennas, Part I—Numerical technique," *IEEE Trans. Antennas and Propagation*, vol. AP-15, pp. 634–639, September 1967.

[10] ——, "Theory of conical equiangular–spiral antennas, Part II—Current distributions and input impedances," *IEEE Trans. Antennas and Propagation*, vol. AP-16, pp. 14–21, January 1968.

[11] G. A. Deschamps, "Scattering diagrams in electromagnetic theory," *Proc. Symp. on Electromagnetic Theory and Antennas* (Copenhagen), pt. 1. New York: Pergamon, 1963.

[12] J. D. Dyson, "The characteristics and design of the conical log-spiral antenna," Antenna Lab., University of Illinois, Urbana, Tech. Rept. 65-4, AFAL-TR-65-124, May 1965.

[13] P. L. Ransom, "An experimental investigation of the four-arm planar logarithmic spiral antenna," Antenna Lab., University of Illinois, Urbana, Tech. Rept. 65-5, AFAL-TR-65-115, May 1965.

[14] Electrical Engineering Research Lab., University of Illinois, Urbana, sec. A(3) of Quart. Rept. 2, Contract AF 33(615)-3216, with Air Force Avionics Lab., February 1966.

[15] O. K. Kim, "An experimental investigation of the conical four-arm logarithmic spiral antenna with large cone angle," Antenna Lab., University of Illinois, Urbana, Tech. Rept. 66-12, AFAL-TR-66-319, September 1966.

[16] S. C. Kuo and C. C. Liu, "Dual polarized center-fed multi-arm spiral monopulse antenna," *1967 IEEE G-AP Internat'l Symp., Digest of Technical Papers* (University of Michigan, Ann Arbor, October 17–19, 1967).

[17] Electrical Engineering Research Lab., University of Illinois, Urbana, sec. A(3) of Quart. Rept. 9, Contract AF 33(615)-3216, with Air Force Avionics Lab., February 1968.

Theoretical and Experimental Studies on the Long Dipole Antenna

CHIN-LIN CHEN, MEMBER, IEEE, AND R. W. P. KING, FELLOW, IEEE

Abstract—**The long transmitting dipole antenna is studied theoretically and experimentally. The Wiener–Hopf technique is used to obtain explicit expressions for the current and charge distributions along the antenna. These quantities are also measured. The theoretical and experimental results are in good agreement.**

I. INTRODUCTION

THE cylindrical dipole is one of the most thoroughly investigated radiating structures. The thin dipole antenna with a half-length h not longer than one wavelength, has been studied theoretically and experimentally by King and his students [1]. The increasing importance of the transient response of a dipole has led to considerable interest in the thin, long, but finite antenna. The thin, infinitely long antenna is well understood [2], [3], [4]. Along it, the current decays as $1/\log k|z|$, where z is the distance from the driving point. This suggests that the current in a long but finite antenna cannot be obtained readily from the solution for an infinitely long antenna. To be useful, the theory for a long but finite antenna has to take account of the successive reflections of the current at the end points. By observing that the vector potential is exceedingly small at points beyond the ends of the antenna, Wu was able to manipulate Hallén's integral equation into a form suitable for the application of the Wiener–Hopf technique [5]. An integral condition was obtained from the vanishing of the current at the ends of the antenna and used to determine the unknown constant C. Once C was known, a somewhat relaxed condition could be used to calculate the characteristics of the antenna. Explicit expressions for the input admittance and

---

Manuscript received May 6, 1968. This research was supported through Joint Services Contract Nonr 1866(32) between Harvard University, the Office of Naval Research, the Signal Corps of the U. S. Army, and the U. S. Air Force.

C.-L. Chen was with the Division of Engineering and Applied Physics, Harvard University. He is now with the School of Electrical Engineering, Purdue University, West Lafayette, Ind.

R. W. P. King is with the Division of Engineering and Applied Physics, Harvard University, Cambridge, Mass.

the radiation patterns of a transmitting antenna were given. Although the procedure for calculating the current and charge distributions along the antenna are suggested in Wu's work, they are not actually evaluated. Since the distributions of current and charge play an important role in understanding the characteristics of the antenna, explicit expressions for these quantities will be presented here.

In Wu's theory for the long antenna, various approximations were made. One crucial step was to replace the Bessel and Hankel functions by the leading terms in their power series expansions. Since this approximation yields a finite input susceptance, even though a delta-function generator is used for exciting the antenna, an inquiry into its physical meaning is suggested. Although Wu subsequently published two papers [6], [7], the mathematical manipulations in them are so complicated that much of the physical meaning is lost. It is, therefore, helpful to review his work with emphasis on its physical meaning, in the hope that it may prove useful for practical applications.

Wu's theory has been confirmed experimentally. The admittance of a long cylindrical antenna with $h < 10\lambda$ was measured by Iizuka, King, and Prasad [8]. Their data agree well with the theoretical values. The current distribution along an antenna with $h < 2\frac{3}{4}\lambda$ was measured by Altschuler [9]. The current distributions along longer antennas have also been measured by Iizuka and King [10]. However, no comparison with the theory was made in either work. Moreover, the measured amplitude and phase were normalized with respect to the driving-point admittance. It can be shown that this is not desirable [11]. Since it is not practical to reduce data from their published results, further measurements of the current distribution have been performed. The charge distribution along a long dipole antenna, which has not been measured before, has also been measured in the present work.

In the next section, the infinite monopole antenna driven successively from a coaxial cable and by a delta-function generator is considered. From a comparison of the two solutions, the physical significance of the various approximations introduced in the mathematical derivation can be studied. The correlation between the theory and experiment is also provided by such a comparison.

In Section III, after a brief review of Wu's theory of the long dipole antenna, explicit expressions for the distributions of current and charge are given. The experimental setup is described in Section IV together with an interpretation of the measured data. A comparison of theoretical and measured results is in the last section.

A more complete set of curves and the Fortran IV program for the computations for the admittance of, and the current and charge distributions in a long dipole antenna are given in the original report [11].

II. A REFLECTION ON ANTENNA THEORY

Since an antenna and a transmission line are integral parts of most radiating systems, any reasonably complete antenna theory must consider the antenna and its feeding structure as a whole. For a cylindrical antenna, either a coaxial line or a two-wire line can be used. However, only the monopole antenna fed by a coaxial cable, as shown in Fig. 1(a), is considered here. Unfortunately, this problem is too difficult to handle rigorously. Instead, the antenna-transmission-line system is studied in three parts: 1) the antenna alone, 2) the transmission line alone, and 3) the coupling between the antenna and the transmission line [1]. The justification for such a decomposition has been discussed by King [1]. Further remarks are in Section II-B. After this separation, the antenna considered is the dipole driven by an idealized delta-function generator shown in Fig. 1(b). Since a delta-function generator can never be realized in practice, it may be wondered how a physical problem, namely a monopole antenna driven by a coaxial line against a ground plane, can be approximated by an unphysical model. To establish this needed connection, and to understand the physical reasoning behind various approximations, two canonical problems must be discussed briefly. Only the physical meaning is emphasized in this section. The mathematical derivations can be found elsewhere [6], [7], [11].

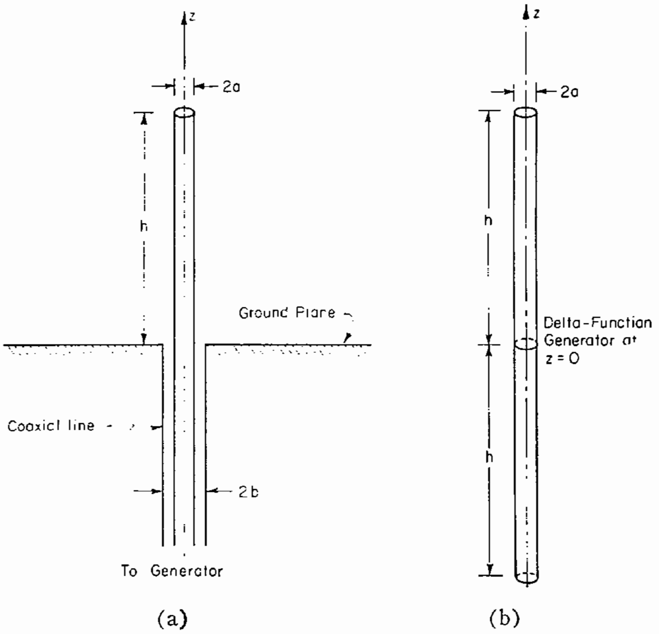

Fig. 1. Antenna models. (a) Monopole driven by a coaxial line. (b) Dipole driven by a delta-function generator.

The cylindrical coordinate system (r, ϕ, z) is used, with the z-axis coincident with the axis of the tubular antenna. A time-harmonic variation of the form $e^{-i\omega t}$ is used and suppressed throughout the work.

A. A Monopole Driven by a Coaxial Line [6], [7]

Consider an infinitely long monopole ($h \to \infty$) driven by a coaxial transmission line over a ground plane. The rotational symmetry of the antenna, coaxial cable, and the method of excitation assure that E_r, E_z, and H_ϕ are the only nonvanishing components of the field. In terms of $E_r(r, 0)$, separate expressions for E_r and H_ϕ may be found for the region above the ground plane and for the coaxial region. An integral equation can then be formulated by requiring H_ϕ to be continuous at $z=0$, and $a<r<b$. For present purposes, it is not necessary to determine $E_r(r, 0)$ explicitly. It is sufficient to note that for $kz \gg 1$, the current distribution along the infinite monopole is

$$I_\infty(z) = \frac{4k}{\pi\zeta_0}\int_a^b E_r(r', 0)dr' \cdot \int_{c_0} \frac{e^{i\zeta z}d\zeta}{\zeta^2\left[1 + \frac{i2}{\pi}\left(\nu + \ln\frac{\xi a}{2}\right),\right]} \tag{1}$$

where ν is Euler's constant, $\xi=(k^2-\zeta^2)^{1/2}$, and the contour C_0 is mainly along the real ζ axis with appropriate indentations at $\zeta=\pm k$; $k=2\pi/\lambda$, $\zeta_0=\sqrt{\mu_0/_0\epsilon}$. The branch cuts are in the first and third quadrants.

From an examination of the expression for the current in the coaxial region, a reflection coefficient due to the geometrical discontinuity at the coaxial line-antenna junction can be found. The apparent admittance as seen from the coaxial line can then be calculated and conveniently split into the following two terms.

$$Y_{a\infty} = 2Y_\infty - i\frac{4ka}{\zeta_0}\frac{1}{A} \tag{2}$$

where A is a function of a/b only and may, therefore, be interpreted as a characteristic of the coaxial line. The last term is the capacitive end correction. Its origin and its physical significance have been discussed by King [1]. Since the first term

$$Y_\infty \frac{2k}{\pi\zeta_0}\int_{C_0} \frac{d\zeta}{\xi^2\left[1 + i\frac{2}{\pi}\left(\gamma + \ln\frac{\xi a}{2}\right)\right]} \tag{3}$$

is a function of ka only, it is natural to interpret $2Y_\infty$ as the intrinsic admittance of an infinitely long monopole driven at its base against a ground plane. In fact, it will be seen in the next section that Y_∞ is exactly the admittance of an infinitely long dipole antenna driven at its center by a delta-function generator. The reason for factoring out a 2 is now clear.

B. Comparison with a Dipole Antenna Driven by a Delta-Function Generator

The analysis of an infinitely long dipole antenna driven by a delta-function generator $V\delta(z)$ (Fig. 1(b)), is comparatively simple. The current distribution is

$$I_{\delta\infty}(z) = \frac{2k}{\pi\zeta_0}V\int_{C_0}\frac{e^{i\zeta z}d\zeta}{\xi^2 J_0(\xi a)H_0^{(1)}(\xi a)}. \tag{4}$$

The input admittance as seen by the delta-function generator is

$$\frac{I_{\delta\infty}(0)}{V} = \frac{2k}{\pi\zeta_0}\int_{C_0}\frac{d\zeta}{\xi^2 J_0(\xi a)H_0^{(1)}(\xi a)}. \tag{5}$$

The input susceptance, or the imaginary part of (5), does not exist owing to the well-known knife edge capacitance and it is due entirely to the idealization of the delta-function generator [12].

It is now expedient to review the motivation for using the delta-function generator. As mentioned earlier, the analysis of the antenna-transmission-line system as a whole is too complicated to yield a useful solution. A decomposition into three parts is possible when $ka<kb\ll 1$, as demonstrated in (2). Strictly speaking, conventional transmission-line theory is valid only for an infinite, and not for a terminated transmission line. In order to apply such a theory to the terminated line, a lumped corrective network is introduced [13]. This takes account both of transmission-line end effects and of the coupling between the antenna and the transmission line. It is represented analytically by the second term in (2). Therefore, an "antenna theory" should be developed to accurately account for the first term of (2), i.e., the intrinsic admittance. The introduction of the delta-function generator is a major step in this direction. However, it is not without drawbacks, owing to the infinite knife edge capacitance. To avoid this difficulty, (4) and (5) are compared with (1)–(3). It is seen that if the Bessel and Hankel functions are approximated by the leading terms in their power series expansions, the corresponding equations are formally identical. It can be shown that the associated expressions for the far field are then also identical. It is therefore necessary to stipulate that all Bessel and Hankel functions are to be replaced by their corresponding power series approximations. Since this stipulation is introduced to remedy the purely local effect of the delta-function generator, it can be used not only for the infinitely long antenna, but also for an antenna of finite length. The subsequent analysis for a long dipole antenna is based on the introduction of the delta-function generator and this stipulation.

III. CURRENT AND CHARGE DISTRIBUTIONS IN A LONG DIPOLE ANTENNA

A. Brief Résumé of Wu's Theory of the Long Antenna

Consider a dipole antenna with half-length h, as shown in Fig. 1(b). It is made of perfectly conducting tubing of radius a with zero wall thickness. It is thin so that $ka\ll 1$. The total current $I(z)$ is along the z-axis, and the vector potential has only one significant component, viz., $A_z(r, z)$. The electric field can be expressed in terms of the vector potential and the boundary condition imposed that requires E_z to vanish at the surface of the conductor at $r=a$, except at the driving point $z=0$ where the delta-function voltage source of unit strength is located. This leads to the following integral equation [1].

$$\int_{-h}^{h} I(z')K(z-z')dz' = \frac{i4\pi}{\zeta_0}\left[C\cos kz + \tfrac{1}{2}\sin k|z|\right], \quad -h \le z \le h \tag{6}$$

where the kernel $K(z)$ is given by

$$K(z) = \frac{1}{2\pi}\int_{-\pi}^{\pi} \frac{exp\left[{}^{ik}\left(z^2 + 4a^2\sin^2\frac{\theta}{2}\right)^{1/2}\right]}{\left[z^2 + 4a^2\sin^2\frac{\theta}{2}\right]^{1/2}}\,d\theta. \tag{7}$$

The unknown constant C is to be determined by the condition

$$I(\pm h) = 0. \tag{8}$$

In order to implement this boundary condition, an accurate description of the field in the neighborhood of $z=h$ is required. Since the antenna is thin, the vector potential in the range $|z|<h$ is relatively large compared to the vector potential in the range $|z|>h$. Furthermore, if the antenna is long, the field near one end is insensitive to a small change in the field near the other end of the antenna. Thus, no appreciable error is introduced, insofar as the field near $z=-h$ is concerned, if the small vector potential in the range, $r=a$, $z>h$ is ignored. For the purpose of determining C, (6) can be replaced by

$$\int_{-h}^{\infty} I(z')K(z-z')dz' = \begin{cases} 0, & z > h \\ \dfrac{i4\pi}{\zeta_0}\left[C\cos kz + \tfrac{1}{2}\sin k|z|\right], & -h < z < h. \end{cases} \tag{9}$$

Note that $I(z)$ must vanish for $z>h$.

This is a Wiener–Hopf integral equation with a displacement kernel. The solution $I(z)$ so obtained is not bounded at $z=-h$ in general, except for a particular choice of the constant C. Hence, an integral condition can be established to determine C. This condition is similar to the edge condition [14] for scattering by a half-plane. The result is [5]

$$C = -\tfrac{1}{2}\,\frac{\sin kh[2T(h) - T(2h)] - \cos kh[2S(h) - S(2h)]}{T(2h)\cos kh + S(2h)\sin kh} \tag{10}$$

where

$$S(X) = \int_{C_0} d\zeta\overline{M}(\zeta)\int_0^{\infty} dze^{-i\zeta z}[\sin kzH(X-z)] \tag{11}$$

$$T(X) = \int_{C_0} d\zeta\overline{M}(\zeta)\int_0^{\infty} dze^{-i\zeta z}[\cos kzH(X-z) - e^{-ikz}] \tag{12}$$

with

$$\overline{M}(\zeta) = \frac{1}{\pi_i J_0(\xi_a)H_0{}^{(1)}(\xi_a)} \cong \frac{1}{2\Omega_1 - \ln\dfrac{\xi^2}{k^2}} \tag{13}$$

and

$$\Omega_1 = \Omega_0 + \frac{i\pi}{2} \tag{14}$$

$$\Omega_0 = \ln\frac{2}{ka} - \gamma. \tag{15}$$

$H(X)$ is the Heaviside function.

The Bessel and Hankel functions in (13) are approximated by the leading terms in their small-argument approximations, in accordance with the stipulation discussed in Section II-B. When this approximated $M(\zeta)$ is used in (11) and (12), explicit expressions for $S(X)$ and $T(X)$ can be obtained for large kX [5]. They are

$$\begin{aligned} 2S(X) \cong{} & -\ln\left[1 + \frac{\pi_i}{(\Omega_0 - \ln 2)}\right] \\ & - \frac{\pi^2}{12}\left[\frac{1}{(\Omega_0 - 2\ln 2)^2} - \frac{1}{(\Omega_0 - 2\ln 2 + \pi i)^2}\right] \\ & + \ln\left[\frac{\Omega_3(X)}{\Omega_2(X)}\right] + \tfrac{1}{2}\gamma'\left[\frac{1}{(\Omega_2(X))^2} - \frac{1}{(\Omega_3(X))^2}\right] \\ & - \frac{i}{2kX}e^{i2kx}\left[\frac{1}{\Omega_2(X)} - \frac{1}{\Omega_3(X)}\right] \end{aligned} \tag{16}$$

$$\begin{aligned} 2iT(X) ={} & +\ln\left[1 + \frac{\pi i}{(\Omega_0 - \ln 2)}\right] \\ & + \frac{\pi^2}{12}\left[\frac{1}{(\Omega_0 - 2\ln 2)^2} - \frac{1}{(\Omega_0 - 2\ln 2 + \pi i)^2}\right] \\ & + \ln\left[\frac{\Omega_3(X)}{\Omega_2(X)}\right] + \frac{\gamma'}{2}\left[\frac{1}{(\Omega_2(X))^2} - \frac{1}{(\Omega_3(X))^2}\right] \\ & + \frac{i}{2kX}e^{i2kX}\left[\frac{1}{\Omega_2(X)} - \frac{1}{\Omega_3(X)}\right]. \end{aligned} \tag{17}$$

The following symbols have been used in (16) and (17).

$$\Omega_2(X) = 2(\Omega_0 - \ln 2) + \ln(2kX) + \gamma - \frac{i\pi}{2} \tag{18}$$

$$\Omega_3(X) = 2(\Omega_0 - \ln 2) + \ln(2kX) + \gamma + \frac{i3\pi}{2} \tag{19}$$

$$\gamma' = \Gamma''(1) - \gamma^2. \tag{20}$$

B. Current Distribution

With C already determined, the current distribution $I(z)$ along the major portion of the antenna can be evaluated by ignoring the vector potential in the range $r=a$, $|z|>h$, where it is small. Thus,

$$\int_{-\infty}^{\infty} I(z')K(z-z')dz' = \begin{cases} \dfrac{i4\pi}{\zeta_0}\left[C\cos kz + \tfrac{1}{2}\sin k|z|\right], & -h<z<h \\ 0, & \text{elsewhere.} \end{cases} \tag{21}$$

The Fourier transform technique can now be initiated by defining $f(z)$ and $\bar{f}(\zeta)$ to be the Fourier transform pair given by

$$\bar{f}(\zeta) = \int_{-\infty}^{\infty} f(z)e^{-i\zeta z}dz \tag{22}$$

$$f(z) = \frac{1}{2\pi}\int_{-\infty}^{\infty} \bar{f}(\zeta)e^{+i\zeta z}d\zeta. \tag{23}$$

The transform of the kernel is well known. In fact, $1/\bar{K}(\zeta)=\overline{M}(\zeta)$ is given in (13). Thus, the solution of (21) is

$$I(z) = \frac{1}{2\pi}\int_{C_0} e^{+i\zeta z}\overline{M}(\zeta)d\zeta \int_{-h}^{h} \frac{i4\pi}{\zeta_0} \cdot \left[C\cos kz' + \tfrac{1}{2}\sin k|z'|\right]e^{-i\zeta z'}dz'. \tag{24}$$

It is now convenient to introduce the function $U(X)$,

$$U(X) = \int_{C_0} \overline{M}(\zeta)d\zeta \int_{-X}^{X} e^{-i\zeta z}\cos kz\, dz \tag{25}$$

and, under the same circumstances that applied in the evaluation of $S(X)$ and $T(X)$, an explicit expression for $U(X)$ can be found for large kX. It is

$$iU(X) = \ln\left[\frac{\Omega_3(X)}{\Omega_2(X)}\right] + \frac{1}{2}\gamma'\left[\frac{1}{(\Omega_2(X))^2} - \frac{1}{(\Omega_3(X))^3}\right] + \frac{i}{2kX}e^{i2kX}\left[\frac{1}{\Omega_2(X)} - \frac{1}{\Omega_3(X)}\right]. \tag{26}$$

In terms of $S(X)$ and $U(X)$, $I(z)$ is given by

$$\begin{aligned} I(z) = \frac{i2}{\zeta_0}\big[&S(h+z)[C\sin kz + \tfrac{1}{2}\cos kz] \\ &+ S(h-z)[-C\sin kz + \tfrac{1}{2}\cos kz] \\ &+ \tfrac{1}{2}U(h+z)[C\cos kz - \tfrac{1}{2}\sin kz] \\ &+ \tfrac{1}{2}U(h-z)[C\cos kz + \tfrac{1}{2}\sin kz] \\ &- S(|z|)\cos kz + \tfrac{1}{2}U(|z|)\sin k|z|\big]. \end{aligned} \tag{27}$$

Due to the approximation made in (21), (27) is not valid for points near the ends, or specifically, $k|z\pm h|<1$. However, since the current should vanish at the ends, a simple extrapolation should be sufficient for this range. If (27) is used in conjunction with (16) and (26), which are valid for large kX only, (27) cannot be used for points near the driving point either. Fortunately, the current at the driving point, and hence the driving-point admittance, can be computed accurately from (27), (16), and (26), and the extrapolation process can again be used.

From (27), the driving-point admittance is given by

$$Y = \frac{I(0)}{1} = \frac{i2}{\zeta_0}[S(h) + CU(h)]. \tag{28}$$

C. Charge Distribution

The continuity equation for charge

$$q(z) = -\frac{i}{\omega}\frac{dI(z)}{dz} \tag{29}$$

may be used to find the charge distribution along the antenna. However, (27), being an asymptotic expression, may not be differentiated without justification. Instead, the integral expression for $I(z)$ should be used. It then follows that

$$q(z) = \frac{i2}{\omega\zeta_0}\int_{C_0} \zeta e^{i\zeta z}\overline{M}(\zeta)d\zeta \int_{-h}^{h} \cdot\left[C\cos kz' + \tfrac{1}{2}\sin k|z'|\right]e^{-i\zeta z'}dz'. \tag{30}$$

This can be expressed in the following form.

$$\begin{aligned} q(z) = -2\epsilon_0\Big\{&\frac{2\pi}{k}(C\cos kh \\ &+ \tfrac{1}{2}\sin kh)[M(h-z) - M(h+z)] \\ &- C\cos kz[S(h+z) - S(h-z)] \\ &+ \frac{C}{2}\sin kz[U(h+z) + U(h-z)] \\ &+ \tfrac{1}{4}\cos kz[U(h+z) - U(h-z)] \\ &+ \tfrac{1}{2}\sin kz[S(h+z) + S(h-z)] \\ &- \tfrac{1}{2}U(z)\cos kz - \sin kz S(|z|)\Big\} \end{aligned} \tag{31}$$

where $M(X)$ is the inverse Fourier transform of $M(\zeta)$, and

$$M(X) = \frac{1}{2\pi}\int_{C_0} \overline{M}(\zeta)e^{i\zeta X}d\zeta \cong \frac{i}{2\pi X}e^{ikX}\left[\frac{1}{\Omega_2(X)} - \frac{1}{\Omega_3(X)}\right] \tag{32}$$

for large kX.

The region of validity of (31) is the same as (27). It is interesting to note that (27) is an even function of z while (31) is an odd function, as expected.

IV. EXPERIMENTAL STUDY

A. Apparatus

An antenna-measuring-line assembly was constructed for measuring the current and the charge distributions in a long monopole driven against a large ground plane with dimensions 24 feet×48 feet. Its basic design is the same as that described by Mack [15]. However, modifications, particularly the guiding tube for the probes, were made to accommodate the unusual length requirement. The conductors of the coaxial line were made of brass tubings, one with $\frac{1}{2}$-inch ID and the other $\frac{1}{4}$-inch OD. The inner conductor could be extended beyond the ground plane to act as the monopole. It had a total length of 12 feet and was slotted to guide the motion of a probe that was attached to a guiding tube. The signal picked up by the probe is fed into a microdot cable that runs inside the guiding tube. To allow the probe to travel over the full length of the antenna without changing the physical length of the microdot cable, it was necessary to construct the guiding tube in two telescoping sections joined by a set screw. Since the inner guiding tube was extremely thin and flexible, the accuracy obtained was not more than ± 0.2 cm in pushing and pulling the tube and the probe. Due to this shortcoming, no accurate admittance measurements were attempted. The detailed construction of the guiding tubes, the feeding stub, the movable short-circuiting plunger, and other auxiliary apparatus can be found in [15].

Polyfoam supports were used to separate the $\frac{1}{4}$-inch brass tubing from the outer conductor of the coaxial line. The relative dielectric constant of the polyfoam is 1.052. This is obtained by measuring the wavelength inside the coaxial line and comparing it with the wavelength measured in a Hewlett–Packard slotted line. Since the antenna conductor was a thin tube with $\frac{1}{4}$-inch OD that could not stand by itself without support when $h>200$ cm, a polyfoam block was again used to provide the needed mechanical support and stability. For short antennas, this polyfoam support had no measurable effect on the current and charge distributions. For longer antennas, the effect of the polyfoam was no longer negligible. This is discussed in Section V.

Two small probes were constructed, one for currents, the other for charges. Their loading effects and symmetry were tested by measuring the standing wave in the short-circuited coaxial cable. A superheterodyne system consisting of a crystal mixer and a 30 MHz IF amplifier was used as the detector that was calibrated with reference to a short-circuited slotted line. The relative phase of the sampled signal was compared with a reference signal. The phase of the reference signal was varied by changing the length of two General Radio trombone-type line stretchers. The line stretchers were connected in series and then terminated by a 50-ohm load, yielding a residue VSWR of 1.05.

B. Normalization

In order to compare the measured relative amplitude and phase with the theoretical results it was necessary to normalize the experimental data. Usually the driving-point current is normalized with respect to the driving-point admittance. This procedure is found to be undesirable by comparing the apparent input admittance with the current at the driving point. A vigorous mathematical proof can be found elsewhere [11], and only a physical explanation is given in the following. The end correction term of (2) represents a lumped correction network to account for the geometrical discontinuity at $z=0$. Due to this discontinuity, the capacitance per unit length $C(z)$ of the coaxial line is not independent of position as for an infinite uniform coaxial line. An accurate determination of the properties of the correction network requires the computation of the variation of $C(z)$ over a distance $10a$ or longer. This detailed calculation and the validity of the end correction are not of present concern. However, it is clear that the end-correction term accounts for the overall effect of the change in the characteristics of the coaxial line over an extended region. On the other hand, a current probe should be extremely small if it is to be useful. Its diameter is usually less than 0.01λ [16] so that signals sampled by it can only represent the local field. Thus, it would not be proper to normalize the driving-point current with respect to the apparent input admittance, unless the second term in (2) is very small.

One may wish to normalize the current with respect to the intrinsic input admittance. However, this is not possible because the signal sampled by the probe does include the effect of the geometrical discontinuity and the end-correction term cannot be separated from the intrinsic input admittance. A possible alternative is to make b/a as small as possible so as to reduce the effect of the second term. However, if the radius of the outer conductor is only slightly larger than that of the inner conductor, a small nonuniformity in the tubing, which is not avoidable, can cause a large change in the characteristics of the coaxial line and hence make the admittance measurement impractical. To avoid these difficulties, a different procedure was adopted. The experimental values of the amplitude and phase of the current at the maximum were compared with the corresponding theoretical computation to determine the normalization factor. A similar procedure was followed for the charge distribution.

V. COMPARISON OF RESULTS AND CONCLUSION

The current distributions along the dipole antennas were measured for various antenna lengths. For the first group of antennas, $2\lambda<h<2\frac{3}{4}\lambda$, the measurements were performed at 600 MHz and 900 MHz. Since the antenna length was less than 150 cm, the experiment could be carried out without polyfoam support. The measured results are in excellent agreement with the theoretical computations based on (27). Two typical results are shown in Figs. 2 and 3. To show the effect of the polyfoam, the current distribution along an antenna with $h=3\lambda$ and with a polyfoam support is shown in Fig. 4. It is seen that the measured current maxima and minima are shifted toward the end of the antenna ($z=h$). These shifts are even more evident for the second group of antennas, $7\lambda<h<8\lambda$, Fig. 5(a), (b), and (c). To demonstrate that they are due entirely to the presence of the polyfoam support, consider a dipole antenna of half-length h situated in a medium characterized by μ_0, ϵ_0. In a rough estimate of the shifts in the maxima and minima, the leading term in the

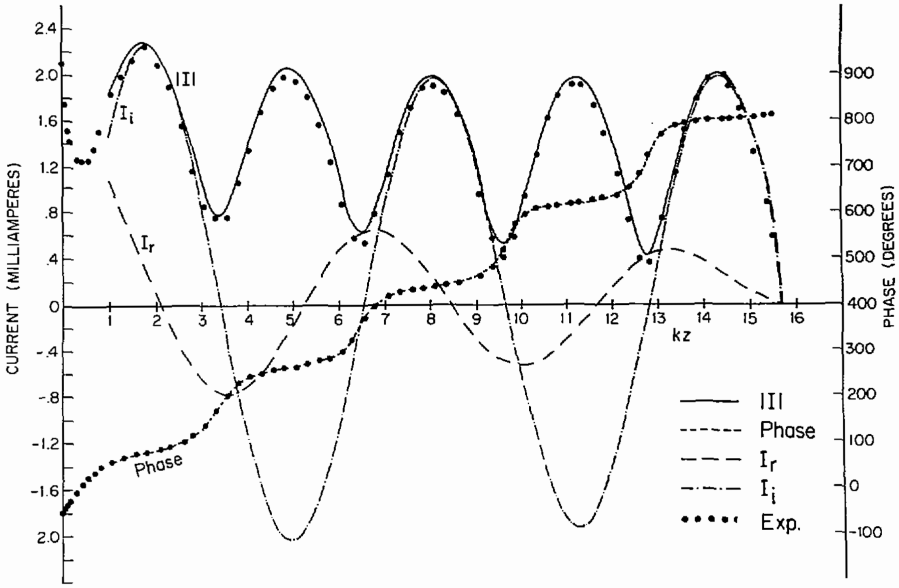

Fig. 2. Distribution of current in long base-driven monopole ($ka = 0.03990$, $kh = 15.7080$, $h/\lambda = 2.5$, $\Omega = 13.34$, without polyfoam support).

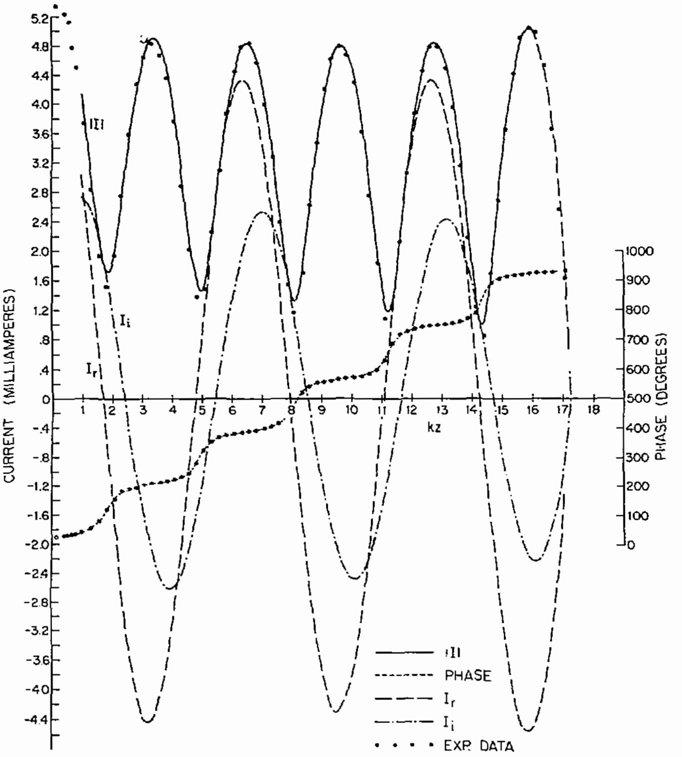

Fig. 3. Distribution of current in long base-driven monopole ($ka = 0.03990$, $kh = 17.2788$, $h/\lambda = 2.75$, $\Omega = 13.53$, without polyfoam support).

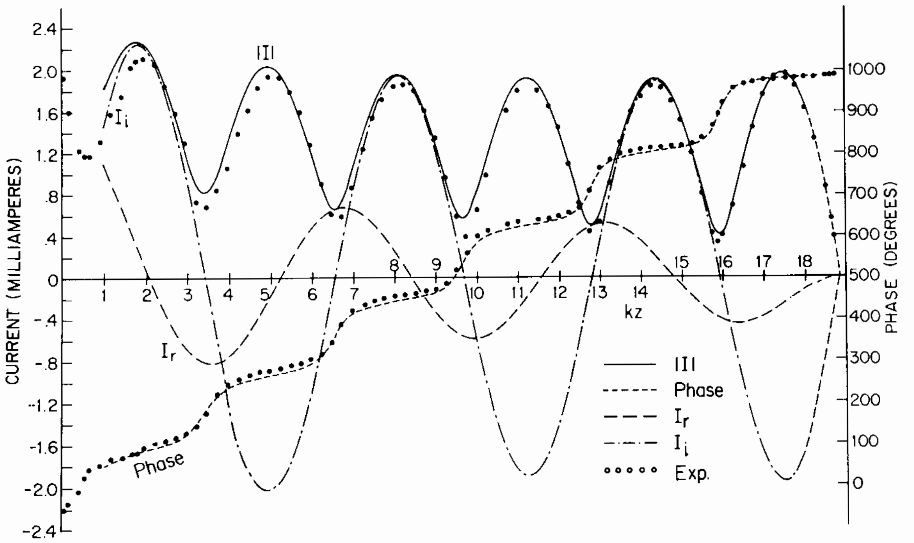

Fig. 4. Distribution of current in long base-driven monopole ($ka = 0.03990$, $kh = 18.8270$, $h/\lambda = 3.0$, $\Omega = 13.70$).

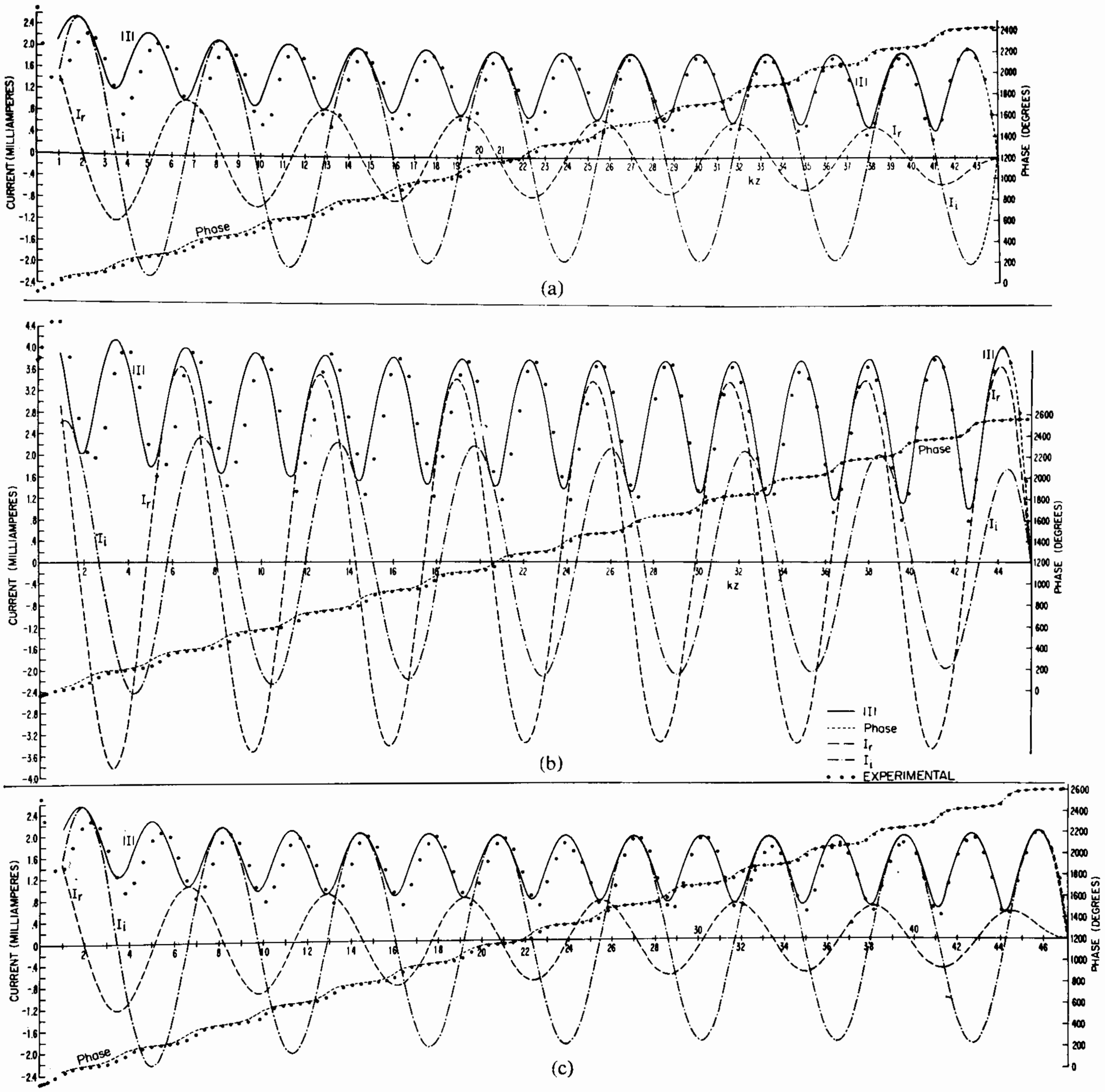

Fig. 5. Distribution of current in long base-driven monopole. (a) ($ka = 0.0623$, $kh = 43.9823$, $h/\lambda = 7.0$, $\Omega = 14.5066$). (b) ($ka = 0.0623$, $kh = 45.5531$, $h/\lambda = 7.25$, $\Omega = 14.57$). (c) ($ka = 0.0623$, $kh = 47.1239$, $h/\lambda = 7.50$, $\Omega = 14.64$).

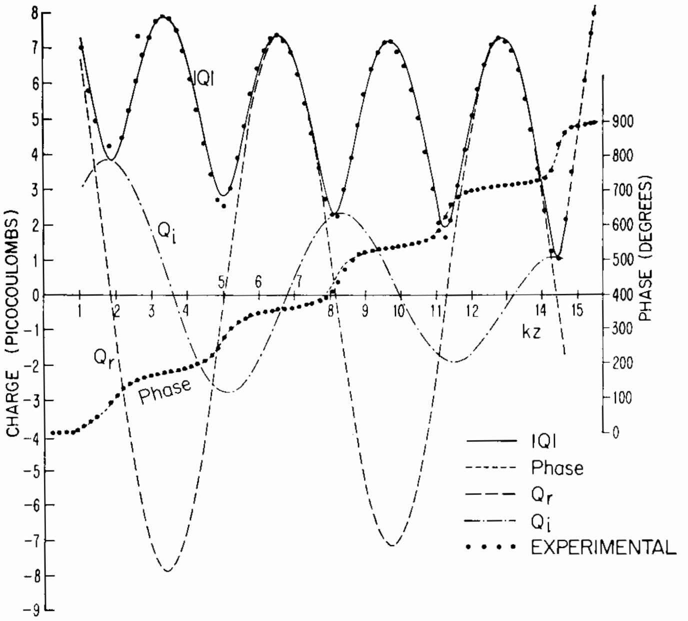

Fig. 6. Distribution of charges in long base-driven monopole ($ka=0.03990$, $kh=15.7080$, $h/\lambda=2.50$, without polyfoam support).

current distribution, viz., $I(z)=I_0 \sin(k|h-z|)$, may be used. The current minima occur at $k|h-z_{n0}|=n\pi$, where n is an integer, z_{n0} is the location of the successive minima, and $k=\omega\sqrt{\mu_0\epsilon_0}$. If the medium is characterized by μ_0, $\epsilon_0(1+\delta)$, then, the minima are located at $k_1|h-z_{n1}|=n\pi$, where $k_1=\omega\sqrt{\mu_0\epsilon_0(1+\delta)}\cong k(1+\frac{1}{2}\delta)$. The shifts in the minima are given by

$$|h - z_{n0}| - |h - z_{n1}| = \frac{n\pi}{k} - \frac{n\pi}{k(1 + \frac{1}{2}\delta)}$$

or

$$k[|h - z_{n0}| - |h - z_{n1}|] = \tfrac{1}{2}\delta n\pi. \qquad (33)$$

The relative dielectric constant of the polyfoam is 1.052, and the antenna tube is half imbedded in the polyfoam block. Thus, it is reasonable to take $\delta=0.025$. When this value of δ is used, the shift of the thirteenth current minimum from the antenna end (not counting the current at $z=h$) is

$$k[|h - z_{13,0}| - |h - z_{13,0}|] \cong 0.50.$$

It is seen from Fig. 6 that this is the right amount of shift. Thus, it is reasonable to conclude that the difference between the experimental results and the theoretical computation is caused by the polyfoam support. The validity of (27) is therefore established.

The charge distributions along the antennas were also measured for five different antenna lengths. The measured results are in agreement with the theoretical computations based on (31), as shown in Figs. 6 and 7(a), (b). When the polyfoam block is used, the charge minima and maxima are again shifted, as observed in Fig. 7(b).

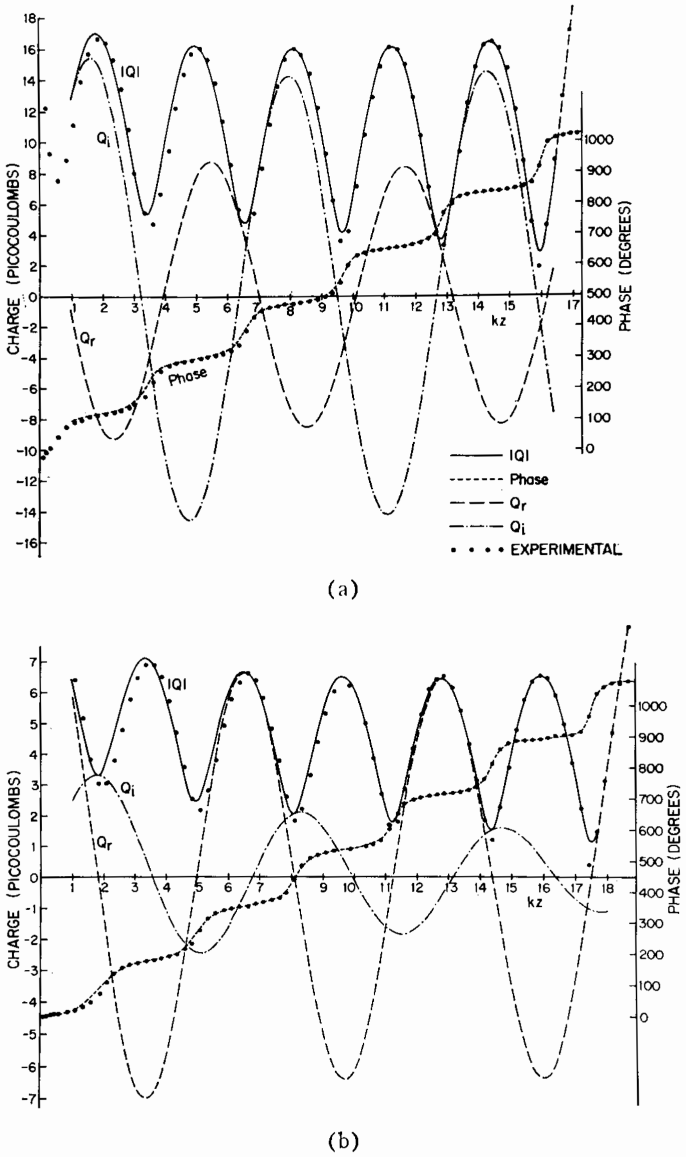

(a)

(b)

Fig. 7. Distribution of charges in long base-driven monopole. (a) ($ka=0.03990$, $kh=17.2788$, $h/\lambda=2.75$). (b) ($ka=0.03990$, $kh=18.8496$, $h/\lambda=3.00$).

Kind and Sandler [17] have observed that for long resonant antennas, the real part of the current behaves like a damped oscillation, as shown in Figs. 2 through 5. It is interesting to note that the imaginary part of the charge has the same behavior. This is to be expected in view of the continuity relation (29) between the charge and the current.

Based on this set of measured data, it is fair to conclude that the current and the charge distributions in long dipole antennas are accurately described by (27) and (31).

ACKNOWLEDGMENT

The authors are indebted to Prof. T. T. Wu for several stimulating discussions. They also wish to thank Mrs. Dilla Tingley for plotting the curves. The apparatus was fabricated by C. Samson and his colleagues.

REFERENCES

[1] R. W. P. King, *The Theory of Linear Antennas*. Cambridge, Mass.: Harvard University Press, 1956.

[2] C. H. Papas, "On the infinitely long cylindrical antenna," *J. Appl. Phys.*, vol. 20, pp. 437–440, 1949.

[3] H. H. Kuehl, "Current on an infinitely long cylindrical antenna," *J. Math. Phys.*, vol. 39, pp. 121–125, 1960.

[4] K. S. Kunz, "Asymptotic behavior of current on an infinite cylindrical antenna," *NBS J. Res.*, vol. 67D, pp. 417–431, 1963.

[5] T. T. Wu, "Theory of the dipole antenna and the two-wire transmission line," *J. Math. Phys.*, vol. 2, pp. 550–574, 1961.

[6] ——, "Input admittance of infinitely long dipole antennas driven from coaxial lines," *J. Math. Phys.*, vol. 3, pp. 1298–1301, 1962.

[7] ——, "Input admittance of linear antennas driven from a coaxial line," *J. Research*, vol. 67D, pp. 83–89, 1963.

[8] K. Iizuka, R. W. P. King, S. Prasad, "The admittance of very long cylindrical antennas," *Proc. IEE* (London), vol. 110, pp. 303–309, 1963.

[9] E. E. Altschuler, "The traveling-wave linear antenna," Ph.D. dissertation, Harvard University, Cambridge, Mass., 1960.

[10] K. Iizuka and R. W. P. King, "The effect of an unbalance on the current along a dipole antenna," *IRE Trans. Antennas and Propagation*, vol. AP-10, pp. 702–707, November 1962.

[11] C. L. Chen, "Theoretical and experimental studies on the long dipole antenna," Div. of Engineering and Applied Physics, Harvard University, Cambridge, Mass., Tech. Rept. 541, 1967.

[12] T. T. Wu and R. W. P. King, "Driving point and input admittance of linear antenna," *J. Appl. Phys.*, vol. 30, pp. 74–76, 1959.

[13] R. W. P. King, *Transmission-line Theory*. New York: Dover, 1965.

[14] J. Meixner, "The edge condition in the theory of electromagnetic waves at perfectly conducting screen," *Ann. Physik*, vol. 6, pp. 2–6, 1949.

[15] R. B. Mack, "A study of circular arrays—Part I: Experimental equipment," Cruft Laboratory, Harvard University, Cambridge, Mass., Tech. Rept. 381, 1963.

[16] H. Whiteside and R. W. P. King, "The loop antenna as a probe," *IEEE Trans. Antennas and Propagation*, vol. AP-12, pp. 291–297, 1964.

[17] R. W. P. King and S. S. Sandler, private communication.

Analysis of Mode Conversion in Waveguide Transition Sections with Surface Impedance Boundaries Applied to VLF Radio Propagation

EZEKIEL BAHAR, MEMBER, IEEE

Abstract—**First- and second-order correction terms are derived for the reflection and transmission scattering coefficients for a step-type transition between two uniform waveguides with surface impedance boundaries. This analysis yields rigorous expressions for the differential transmission and reflection coefficients defined for an infinitesimal step transition. These coefficients are essential in the derivation of the coupled differential equations for the wave amplitudes in a transition section of gradually varying height.**

I. INTRODUCTION

THEORETICAL investigations of the effects of mode conversion on VLF radio propagation in the nonuniform earth-ionosphere waveguide have led to a clearer understanding of the diurnal phase and amplitude variations of the VLF signals [1]–[3].

In the two-dimensional treatment of this problem, the boundaries of the curved earth–ionosphere waveguide are characterized by finite surface impedances. This two-dimensional treatment is justified on the basis of an analysis of the problem by Wait [4]. In these investigations, the waveguide is assumed to have an abrupt change of height to represent an idealized day-to-night transition of the effective ionosphere height. In the analysis by Bahar [2], in which reflections are not neglected, limiting expressions are derived for these mode conversion coefficients for transition sections with infinitesimal height variations. These expressions are identified as differential transmission and reflection coefficients. These coefficients are in turn used to derive a set of coupled first-order differential equations for the forward and backward wave amplitudes in a transition region of arbitrarily varying effective height. In such an analysis the transition section is regarded as consisting of an infinite number of elementary uniform waveguide sections cascaded together.

Recently Wait [3] has suggested that the transition region between two uniform waveguides may be regarded as consisting of a finite number of step-type transition sections cascaded together. Using this approach, the change in height at the transition plane between the subsections of the waveguide is obviously also finite. With this model, the mode conversion coefficients for the entire transition section are a product of the transmission scattering matrices of the subsections, provided that reflections are neglected.

Manuscript received May 24, 1968.

The author is with the Department of Electrical Engineering, University of Nebraska, Lincoln, Neb.